Journal of Non-Newtonian Fluid Mechanics, 24 (1987) 67–83
Elsevier Science Publishers B.V., Amsterdam – Printed in The Netherlands

HYPERBOLICITY AND CHANGE OF TYPE IN THE FLOW OF VISCOELASTIC FLUIDS THROUGH PIPES

M. AHRENS

Department of Aerospace Engineering and Mechanics, University of Minnesota, Minneapolis, MN 55455 (U.S.A.)

Y.J. YOO

Department of Mechanical Engineering, College of Engineering, Seoul National University, Seoul 151 (Korea)

and D.D. JOSEPH

Department of Aerospace Engineering and Mechanics, University of Minnesota, Minneapolis, MN 55455 (U.S.A.)

(Received August 21, 1986)

Summary

We consider the steady flow of an upper convected Maxwell fluid through a pipe with wavy walls. The analysis is an extension to round pipes of the methods introduced by Yoo and Joseph [1] to study the same problem in plane channels. As in the channel problem, the vorticity in a small cylinder at the center of the pipe becomes hyperbolic when the centerline velocity is larger than the speed of shear waves into rest. The region of hyperbolicity is smaller, but the decay of vorticity is less, when the elasticity parameter is larger.

1. Introduction

This work is an extension of the analysis given by Yoo and Joseph [1] for channels to the same problem for round pipes. The history of this problem and nearly all of the qualitative results can be found in [1] and will not be repeated here. We take note of the following differences between the problems.

0377-0257/87/$03.50

We use a different scale to non-dimensionalize the stresses, which leads us to an extra factor W, the Weissenberg number, in front of every stress variable. There are of course extra lower order terms when the equations are written in polar coordinates. These extra terms give rise to terms with singular factors proportional to r^{-1} and r^{-2}. These singular factors give rise to difficulties in the numerical solution which we have avoided by computing directly from the first order quasilinear system (2.1) rather than the stream function equation used in [1].

It is necessary to call attention to the fact that the analysis of characteristics in the linear approximation does not depend on the type of perturbation of Poiseuille flow, provided it is small. Though we do analyze wavy walls, the characteristics for the vorticity would be the same for any other problem. We are obliged then to consider the relevance of the analysis of the type of a partial differential equation for the flow near the exit of a pipe from which a viscoelastic fluid is extruded. The experiments of Joseph, Matta, and Chen [2] do suggest a strong dependence on a change of type correlated with the viscoelastic Mach number; but apart from this the relation of this analysis to those experiments is obscure. The appendix of this paper discusses the characteristics for perturbations of uniform flow, which is relevant for the flow after the pipe exit (see also [2], section 5).

2. Governing equations

We consider the steady flow of an incompressible upper convected Maxwell fluid through a pipe whose radius varies sinusoidally along the axis. The equations governing this flow are

$$\operatorname{div} \boldsymbol{u} = 0,$$

$$\rho \boldsymbol{u} \nabla \boldsymbol{u} = -\nabla p + \nabla \tau,$$

$$\lambda\left[\boldsymbol{u}\nabla\tau - \nabla\boldsymbol{u}\tau - \tau\nabla\boldsymbol{u}^{\mathrm{T}}\right] + \tau = \eta(\nabla\boldsymbol{u} + \nabla\boldsymbol{u}^{\mathrm{T}}), \tag{2.1}$$

where ρ is the density, λ is the relaxation time, η is the viscosity, $\boldsymbol{u}$ is the velocity, p is the constitutively indeterminate part of the Cauchy stress tensor, and τ is the determinate part.

In the analysis we will assume axisymmetric flow. Hence, in cylindrical polar coordinates, all dependent variables are independent of the polar angle θ, and there is no velocity or shear stress in the θ direction.

A list of symbols used in the analysis are:

(r, z)	radial and axial coordinates for the pipe
b	mean pipe radius
(u, w)	components of velocity: $\boldsymbol{u} = u\boldsymbol{e}_r + w\boldsymbol{e}_z$
w_0	centerline ($r = 0$) velocity

$(\sigma_1, \sigma_2, \sigma_3, \tau)$ components of the determinate stress:

$$\tau = \sigma_1 e_r e_r + \sigma_2 e_\theta e_\theta + \sigma_3 e_z e_z + \tau(e_r e_z + e_z e_r)$$

R Reynolds number $= \rho w_0 b/\eta$
W Weissenberg number $= \lambda w_0/b$
E elasticity number $= \eta\lambda/\rho b^2$
M viscoelastic Mach number $= w_0/(\eta/\lambda\rho)^{1/2}$

Note that E is a material parameter, and the shear wave speed

$$c = (\eta/\lambda\rho)^{1/2} \tag{2.2}$$

is also a material parameter. Of the four parameters R, W, E, M, only two are independent, since

$$M^2 = RW \tag{2.3a}$$

and

$$W = RE. \tag{2.3b}$$

Newtonian fluids arise in the limit $\lambda \to 0$ for finite fixed values of the viscosity η. In this limit, $c \to \infty$, $M \to 0$, $E \to 0$ in such a way that

$$R = M/E^{1/2} \tag{2.4}$$

remains finite.

The boundary value problem for our problem is the system (2.1) together with no-slip conditions at the wall of the pipe

$$u = w = 0 \text{ at } r = b(1 + \epsilon \sin nz), \tag{2.5}$$

where ϵ is the amplitude perturbation of the sinusoidal variation of period $2\pi/n$ of the wall. We assume flow symmetry about the centerline

$$u = \frac{\partial w}{\partial r} = 0 \text{ at } r = 0, \tag{2.6}$$

and that all flow variables are periodic in the axial direction z.

We solve this problem by considering a linear perturbation of Poiseuille flow. We first compute the solution for Poiseuille flow when $\epsilon = 0$. We then derive and solve a perturbed problem for $0 < \epsilon \ll 1$, using the technique of domain perturbation (see Yoo and Joseph [1]). We consider only the first order perturbation here. The perturbed problem will be linear and of mixed type; that is, if $M > 1$, then in a region near the centerline of the pipe the vorticity equation will be hyperbolic, and elliptic elsewhere.

3. Poiseuille flow

By a Poiseuille flow we mean a solution of the form

$$u = 0, \quad w = w(r) \tag{3.1a}$$

in a pipe with straight walls, $\epsilon = 0$. We also assume a constant axial pressure gradient

$$\frac{\partial p}{\partial z} = -k^2, \tag{3.1b}$$

and that the stress components σ_1, σ_2, σ_3, and τ are functions of r only. A solution of system (2.1) and boundary conditions (2.5) and (2.6) for $\epsilon = 0$ is

$$\begin{aligned} &u = 0, \\ &w = \frac{k^2 b^2}{4\eta}\left(1 - \frac{r^2}{b^2}\right), \\ &p = -k^2 z + \text{constant}, \\ &\sigma_1 = \sigma_2 = 0, \\ &\sigma_3 = \frac{\lambda k^4}{2\eta} r^2, \\ &\tau = -k^2 r/2. \end{aligned} \tag{3.2}$$

Using b, $w_0 = w(0) = k^2 b^2/4\eta$, and $bk^2/4$ as characteristic values for lengths, velocities, and stresses, respectively, we can write (3.2) in the non-dimensional form

$$\begin{aligned} &u = \sigma_1 = \sigma_2 = 0, \\ &w = 1 - r^2, \\ &p = -4z + \text{constant}, \\ &\sigma_3 = 8Wr^2, \\ &\tau = -2r. \end{aligned} \tag{3.3}$$

We are using the same symbols for the physical variables in (3.2) and the non-dimensional variables in (3.3), and we will rely on the context to make our intention clear.

4. Characteristics for the vorticity

Before continuing with the perturbation problem, we remark on the change of type of system (2.1). Using the scales introduced after (3.2) we

may write the dimensionless form of the system (2.1) for axisymmetric problems as a quasilinear system:

$$\boldsymbol{A}(\boldsymbol{g})\frac{\partial \boldsymbol{g}}{\partial r}+\boldsymbol{B}(\boldsymbol{g})\frac{\partial \boldsymbol{g}}{\partial z}=\boldsymbol{f}(\boldsymbol{g}), \tag{4.1a}$$

where

$$\boldsymbol{g}=(u,\ w,\ p,\ \sigma_1,\ \sigma_2,\ \sigma_3,\ \tau), \tag{4.1b}$$

$$\boldsymbol{A}=\begin{vmatrix} 1 & 0 & 0 & 0 & 0 & 0 & 0 \\ Ru & 0 & 1 & -1 & 0 & 0 & 0 \\ 0 & Ru & 0 & 0 & 0 & 0 & -1 \\ -2(W\sigma_1+1) & 0 & 0 & Wu & 0 & 0 & 0 \\ 0 & 0 & 0 & 0 & Wu & 0 & 0 \\ 0 & -2W\tau & 0 & 0 & 0 & Wu & 0 \\ 0 & -(W\sigma_1+1) & 0 & 0 & 0 & 0 & Wu \end{vmatrix} \tag{4.1c}$$

$$\boldsymbol{B}=\begin{vmatrix} 0 & 1 & 0 & 0 & 0 & 0 & 0 \\ Rw & 0 & 0 & 0 & 0 & 0 & -1 \\ 0 & Rw & 1 & 0 & 0 & -1 & 0 \\ -2W\tau & 0 & 0 & Ww & 0 & 0 & 0 \\ 0 & 0 & 0 & 0 & Ww & 0 & 0 \\ 0 & -2(W\sigma_3+1) & 0 & 0 & 0 & Ww & 0 \\ -(W\sigma_3+1) & 0 & 0 & 0 & 0 & 0 & Ww \end{vmatrix} \tag{4.1d}$$

and

$$\boldsymbol{f}=\begin{vmatrix} -u/r \\ (\sigma_1-\sigma_2)/r \\ \tau/r \\ -\sigma_1 \\ 2(W\sigma_2+1)u/r-\sigma_2 \\ -\sigma_3 \\ -(Wu/r+1)\tau \end{vmatrix} \tag{4.1e}$$

The characteristic curves of such a quasilinear first order system are given by (see Joseph, Renardy, and Saut [3])

$$\det\left[\boldsymbol{A}-\boldsymbol{B}\frac{\mathrm{d}r}{\mathrm{d}z}\right]=0. \tag{4.2}$$

That is,

$$\left[u-w\frac{\mathrm{d}r}{\mathrm{d}z}\right]^3\left[\left(\frac{\mathrm{d}r}{\mathrm{d}z}\right)^2+1\right]\left[a_2\left(\frac{\mathrm{d}r}{\mathrm{d}z}\right)^2+2a_1\frac{\mathrm{d}r}{\mathrm{d}z}+a_0\right]=0, \tag{4.3a}$$

where

$$a_0 = M^2 w^2 - W\sigma_3 - 1,$$

$$a_1 = M^2 uw - W\tau,$$

$$a_2 = M^2 u^2 - W\sigma_1 - 1. \tag{4.3b}$$

Hence there are always real characteristics

$$\frac{dr}{dz} = \frac{u}{w},$$

which are streamlines, and imaginary characteristics

$$\frac{dr}{dz} = \pm i.$$

The streamline characteristics may be associated with the convective derivative, and the imaginary characteristics may be associated with the incompressibilty condition.

The remaining pair of characteristic curves are determined by

$$\frac{dr}{dz} = -\frac{a_1}{a_2} \pm \frac{(a_1^2 - a_2 a_0)^{1/2}}{a_2}, \tag{4.4}$$

and these are real if and only if

$$a_1^2 - a_2 a_0 = (M^2 uw - W\tau)^2 - (M^2 w^2 - W\sigma_3 - 1)(M^2 u^2 - W\sigma_1 - 1) > 0. \tag{4.5}$$

There is therefore the possibility of a change of type from imaginary to real characteristics in crossing from one region of the flow to another, depending on the local relative magnitudes of the velocities and stresses in (4.5).

The characteristics given by (4.4) may be associated with the vorticity equation. A routine manipulation to derive the vorticity equation from system (4.1) gives the form

$$a_2 \frac{\partial^2 \zeta}{\partial z^2} + 2a_1 \frac{\partial^2 \zeta}{\partial r \partial z} + a_0 \frac{\partial^2 \zeta}{\partial r^2} = g, \tag{4.6}$$

where a_2, a_1, and a_0 are given in (4.3b), ζ is the non-zero component of vorticity ($\zeta = \text{curl } \boldsymbol{u} = \zeta e_\theta$), and g is a function of the flow variables and their first and second derivatives, which includes ζ and its first derivatives. Thus the vorticity equation is locally hyperbolic if condition (4.5) holds, or elliptic if the inequality in (4.5) is reversed. In regions of the flow where (4.6) is hyperbolic, there is the possibility that the derivatives of the vorticity may be discontinuous across the characteristics given by (4.4).

The results of this section, so far, apply to any axisymmetric problem, linear or non-linear, and not just to the problem introduced in section 2. Since the problem of section 2 does not have discontinuous boundary data, we do not expect to discover discontinuities of the vorticity derivatives in the hyperbolic region of the flow.

For definiteness, let us now consider a perturbation of the Poiseuille flow solution given in section 3. That is, we may write $\boldsymbol{g} = \boldsymbol{g}_0 + \boldsymbol{g}_1$, where $\boldsymbol{g}_0$ is the Poiseuille flow variables and $\boldsymbol{g}_1$ is any perturbation. The linearization of system (4.1) would take the form

$$\boldsymbol{A}(\boldsymbol{g}_0)\frac{\partial \boldsymbol{g}_1}{\partial r} + \boldsymbol{B}(\boldsymbol{g}_0)\frac{\partial \boldsymbol{g}_1}{\partial z} = \boldsymbol{f}_1(\boldsymbol{g}_1; \boldsymbol{g}_0). \tag{4.7}$$

That is, $\boldsymbol{A}$, $\boldsymbol{B}$ are given by (4.1c, d) with all variables given by the Poiseuille flow (3.3). Here $\boldsymbol{f}(\boldsymbol{g}_1; \boldsymbol{g}_0)$ represents the linearization of $\boldsymbol{f}(\boldsymbol{g})$. The characteristics given by (4.4) represent characteristics for the $\boldsymbol{g}_1$, and may be found by substituting the solution (3.3) into (4.4):

$$\frac{\mathrm{d}r}{\mathrm{d}z} = 2Wr \pm \left[M^2(1-r^2)^2 - 4W^2r^2 - 1\right], \tag{4.8}$$

with the condition (4.5) for real characteristics becoming

$$M^2(r^2-1)^2 - 4W^2r^2 - 1 > 0. \tag{4.9}$$

This condition always fails near $r = 1$; but is satisfied near $r = 0$, provided $M^2 - 1 > 0$. Hence there is a region near the centerline of the pipe for which the perturbed vorticity equation is hyperbolic, if $M > 1$; and a region of ellipticity near the wall. The radius at which the change of type occurs is found from (4.9) to be

$$r^* = (1+2E)^{1/2}\left[1 - \left[1 - (M^2-1)M^{-2}(1+2E)^{-2}\right]^{1/2}\right]^{1/2}. \tag{4.10}$$

In the next section we return to the pipe flow with wavy walls discussed in section 2. The linearized problem derived will have characteristics given by (4.8), with a region $0 < r < r^*$ in which the perturbed vorticity satisfies a hyperbolic equation (for $M > 1$), and a region $r^* < r < 1$ in which it satisfies an elliptic equation.

5. Linearized problem for pipe flow with wavy walls

The problem for the steady flow of an upper convected Maxwell fluid through a periodically constricted pipe is governed by system (2.1) (non-dimensionalized as in (4.1)) with boundary values (2.5) and (2.6) in the domain

$$V_\epsilon = \{(r, z): z \in (-\infty, \infty),\ r \in [0, 1 + \epsilon \sin nz]\}. \tag{5.1}$$

There is a one-to-one map of V_ϵ from the straight wall pipe

$$V_0 = \{(r_0, z_0): z_0 \in (-\infty, \infty), r_0 \in [0, 1]\} \tag{5.2}$$

given by

$$z = z_0, \tag{5.3}$$

$$r = r_0(1 + \epsilon \sin nz_0).$$

To solve the problem we use the technique of domain perturbation (see Yoo and Joseph [1]), and solve the first order perturbation problem. Thus, the flow variables (4.1b) may be written as

$$\boldsymbol{g}(r, z, \epsilon) = \boldsymbol{g}^{[0]}(r_0, z_0) + \epsilon \boldsymbol{g}^{[1]}(r_0, z_0) + O(\epsilon^2), \tag{5.4}$$

where

$$\boldsymbol{g}^{[1]}(r_0, z_0) = \frac{\mathrm{d}}{\mathrm{d}\epsilon}\boldsymbol{g}(r, z, \epsilon)\,|_{\epsilon=0} = \boldsymbol{g}^{\langle 1\rangle}(r_0, z_0) + \left.\frac{\partial r}{\partial \epsilon}\right|_{\epsilon=0} \frac{\partial \boldsymbol{g}^{[0]}}{\partial r_0}, \tag{5.5}$$

and where

$$\boldsymbol{g}^{\langle 1\rangle}(r_0, z_0) = \frac{\partial}{\partial \epsilon}\boldsymbol{g}(r, z, \epsilon)\,|_{\epsilon=0}, \tag{5.6a}$$

and

$$\left.\frac{\partial r}{\partial \epsilon}\right|_{\epsilon=0} = r_0 \sin nz_0. \tag{5.6b}$$

Of course, the zeroth order variables are precisely the Poiseuille variables given by (3.3).

The problem for the fist order perturbation is found by simply taking the derivative with respect to ϵ, and evaluating at $\epsilon = 0$, of system (4.1) and of the boundary conditions (2.5) and (2.6). For simplicity of notation, we will drop the subscripts of 0 on (r_0, z_0), and we will not use the superscript $\langle 1\rangle$ for the flow variables. With these notations, the problem for the first order flow variables $\boldsymbol{g}^{\langle 1\rangle}(r_0, z_0)$ is the system of PDE's

$$\begin{aligned}
&u_r + w_z = -u/r,\\
&R(1-r^2)u_z + p_r - (\sigma_{1r} + \tau_z) = (\sigma_1 - \sigma_2)/r,\\
&R\left[(1-r^2)w_z - 2ru\right] + p_z - (\tau_r + \sigma_{3z}) = \tau/r,\\
&W\left[(1-r^2)\sigma_1 + 4ru_z\right] - 2u_r = -\sigma_1,\\
&W(1-r^2)\sigma_{2z} = -2u/r - \sigma_2,\\
&W\left[(1-r^2)\sigma_{3z} + 4rw_r\right] - 2(8W^2r^2 + 1)w_z = -\sigma_3 - 4Wr(\tau + 4Wu),\\
&W(1-r^2)\tau_z - (8W^2r^2 + 1)u_z - w_r = -\tau + 2W(2u - r\sigma_1),
\end{aligned} \tag{5.7a}$$

together with the boundary conditions

$$u = 0; \quad w = 2 \sin nz \text{ at } r = 1, \tag{5.7b}$$

and

$$u = w_r = 0 \text{ at } r = 0. \tag{5.7c}$$

In (5.7), subscripts of r and z denote partial derivatives. In addition, the perturbation of the vorticity equation may be written as

$$\begin{aligned}\left[M^2(1-r^2)^2 - 8W^2r^2 - 1\right]\zeta_{zz} + 4Wr\zeta_{rz} - \zeta_{rr} &= -\left[R(1-r^2) + 6W\right]\zeta_z \\ &+ 2W\left[w_{rz} + u_{zz} + 3\sigma_{1r} - 8Wrw_{zz} - r(\sigma_{1rr} - \sigma_{3zz})\right] \\ &- (w_{rr} + w_{zz})/r - (2u_z - w_r + 4Wu)/r^2. \end{aligned} \tag{5.8}$$

In section 4 we noted that the system (5.7) has characteristics given by (4.3), and the vorticity equation (5.8) has characteristics given by (4.8). There is a change of type from hyperbolic to elliptic at r^* given by (4.10) provided that $M > 1$.

The linear system (5.7) was solved numerically, after first reducing it to a system of ODE's. The system of ODE's arose by a separation of variables of the form

$$\boldsymbol{g}(r, z) = \boldsymbol{g}_1(r) \cos nz + \boldsymbol{g}_2(r) \sin nz, \tag{5.9}$$

where $\boldsymbol{g} = (u, w, p, \sigma_1, \sigma_2, \sigma_3, \tau)$ is the vector of perturbation variables. The form of (5.9) makes explicit the assumed periodicity of all flow variables; which combined with the boundary conditions (5.7b,c), is sufficient to complete the determination of the first order perturbation.

The system of ODE's was solved numerically by using an available IMSL routine, DVCPR, on the Cyber mainframe system at the University of Minnesota. This routine is a finite difference routine for a system of ODE's with two-point boundary data, with the grid points chosen adaptively in order to make local errors approximately the same size everywhere. The solution was checked by also using a multiple shooting routine provided in the IMSL package, routine DTPTB. The results agreed. Further, the problem solved by Yoo and Joseph [1] was also solved by the finite difference and multiple shooting routines, with excellent agreement. In passing, we note that the finite difference routine was the most efficient, using on the average only 10–20% of the time required by the shooting methods.

6. Results

The characteristics of the perturbed vorticity, as given by (4.8) in the region $0 < r < r^*$, are precisely the same as for channel flow, with (x, y)

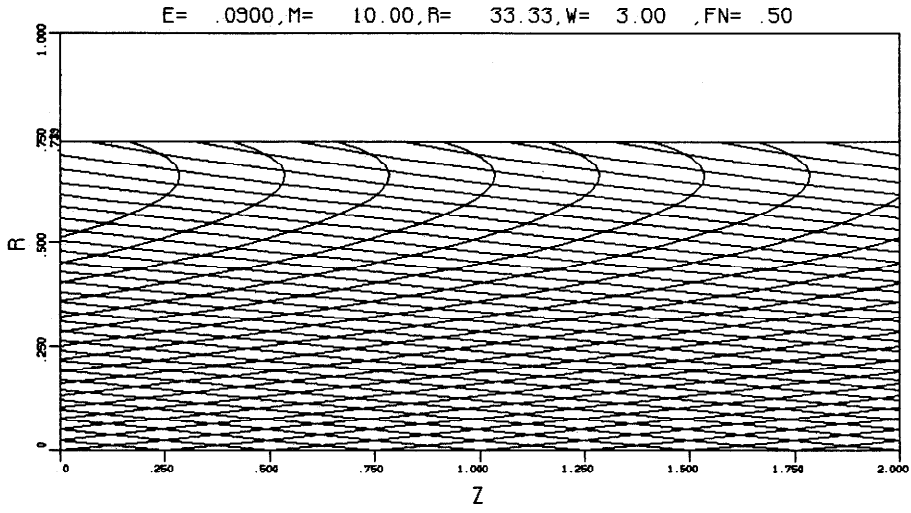

Fig. 1. Characteristics.

replaced with (z, r). Thus we refer the reader interested in further discussion of the characteristics to the work of Yoo and Joseph [1], especially their section 4, where graphs of the characteristics for several cases are displayed.

Here we display a graph of the characteristics, in Fig. 1, for parameter values also used in Figs. 2 and 6. The value of r^* is indicated in the figure, and both sets of characteristics of (4.8) are drawn.

In general, the results of the perturbed pipe problem are similar to the results of the channel problem of Yoo and Joseph [1]. The isovorticity curves presented there are like the isovorticity curves of pipe flow with the same values of M, E, and n. In addition, we have plotted contours of constant perturbed stress for both the channel and the pipe problems, again with similar graphs for corresponding parameter values. We found that the stresses are slightly larger in the pipe flow case, about 10–20% larger.

A particularly striking feature of both problems is the behavior of the vorticity for different values of E. When $M > 1$ is fixed, the vorticity in the hyperbolic region oscillates (see Yoo and Joseph [1]). For larger values of E, the oscillations are not damped as r decreases to zero. This feature appears in the isovorticity plots as isolated regions of positive and negative vorticity, with little change in maximum absolute value. This is seen in Fig. 2 (see also [1]). For small E, however, the oscillations are damped severely as r decreases. In fact, the perturbed vorticity nearly vanishes in the center of the pipe. To make this more apparent, we have graphed the vorticity in the separated form

$$\zeta^{[1]}(r_0, z_0) = \zeta_1(r_0) \cos nz_0 + \zeta_2(r_0) \sin nz_0. \tag{6.1}$$

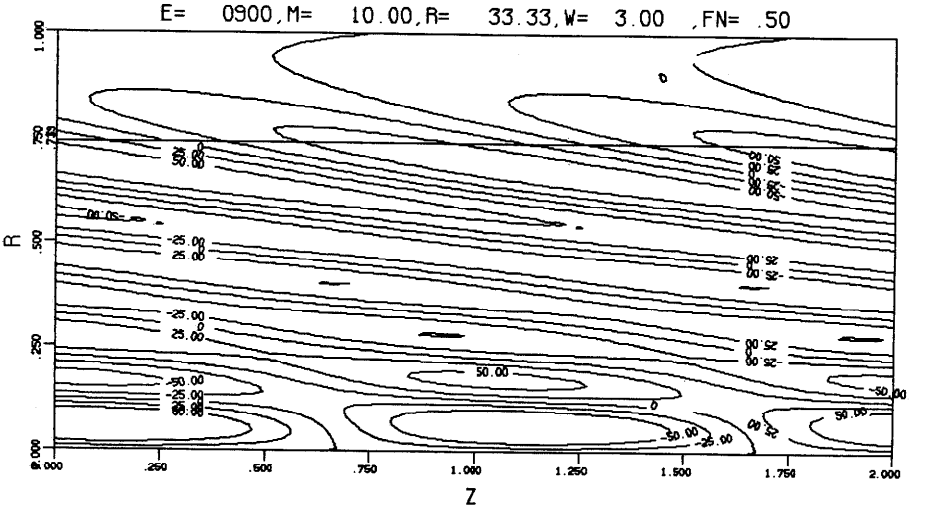

Fig. 2. Isovorticity curves.

In Figs. 3–6 we present graphs of $\zeta_1(r_0)$ for various values of E. In those figures $FN = n/2\pi = 1/2$ is fixed, and ζ_1 is labelled VOR1. Notice the strong decay of the vorticity for small E, Figs. 3–5, and the lack of decay for larger values of E, Fig. 6. Also clear from these graphs is the observation, noted already by Yoo and Joseph [1], that the oscillations have a period governed by M. That is, in Fig. 5, where $M = 20$, the interval between the zeroes of the oscillations is nearly precisely half that in Figs. 4 and 6, where $M = 10$. This can be shown from the vorticity equation (5.8) by assuming $M > 1$ and $W = ME^{1/2} < O(1)$, and keeping only terms of highest order in powers of $1/M$. In performing the expansions the radial derivatives are scaled with M, in accordance with the observation of the period; that is,

$$\zeta_{r*} = 1/M\, \zeta_r. \tag{6.2}$$

After using the separation (6.1), we find the following pair of equations

$$\zeta_1'' + n^2(1-r^2)\zeta_1 - \frac{n(1-r^2)^2}{W}\zeta_2 = O(1/M),$$

$$\zeta_2'' + n^2(1-r^2)\zeta_2 + \frac{n(1-r^2)^2}{W}\zeta_1 = O(1/M). \tag{6.3}$$

We take $1-r^2$ to be constant and look for exponential solutions for ζ_1 and ζ_2. This leads to

$$\zeta_1, \zeta_2 \sim \exp(\lambda r), \tag{6.4}$$

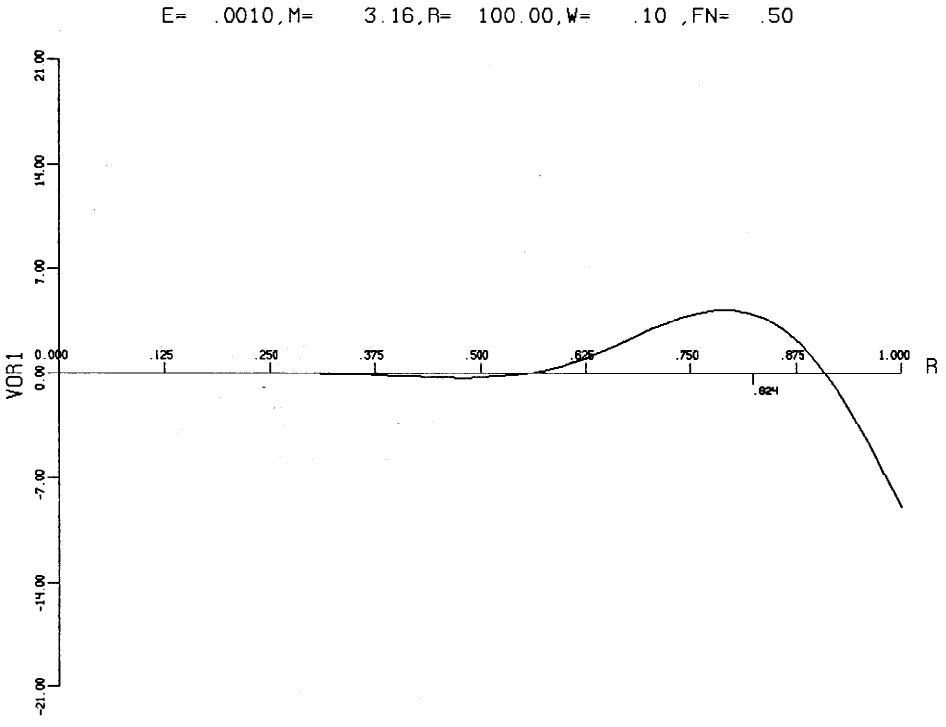

Fig. 3. Pipe flow vorticity.

where

$$\lambda = E^{-1/2}/2 + n(1 - r^2)M\mathrm{i}. \tag{6.5}$$

Hence, the vorticity has a period of about

$$2\pi/n(1 - r^2)M, \tag{6.6}$$

which for the value $n = \pi$, and $1 - r^2 = 1$, agrees very well with Figs. 3–6. In addition, the perturbed vorticity decays, as r decreases, by the exponential rate governed by $E^{-1/2}/2$. This agrees with the observation that the damping is most rapid for small E. This damping factor also agrees, though only approximately so, with the measurements of the damping taken from Figs. 3–6.

The lack of decay of the vorticity for larger values of E, coupled with the fact that the values of the vorticity are larger for larger E, gives large gradients of vorticity. These large gradients prohibit computing solutions for larger values of E. In fact, the acceptable limit on computing costs limited computations to $W = ME^{1/2} < 3$. For the corresponding channel flow problem the limit was $W < 7$.

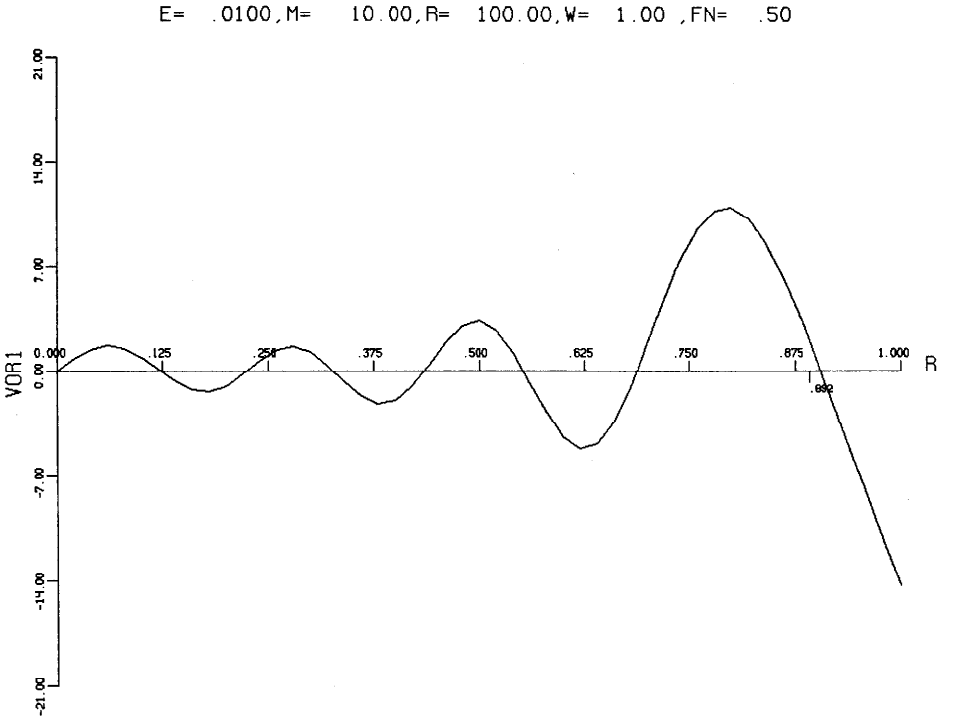

Fig. 4. Pipe flow vorticity.

An attempt to further use the idea of the change of type of the vorticity equation for Poiseuille flow was made by trying to correlate the data from some recent experiments on the die swell phenomena by Joseph, Matta, and Chen [2]. They found that when the flow rate through a die is larger than some critical rate, the initial swelling of the extruded material does not occur at the end of the die, but is delayed to a position further downstream. The appearance of the swell is much like an hydraulic jump. If one assumes that the dynamics can be related to a perturbation of Poiseuille flow at the pipe exit, then the characteristics of the vorticity equation in the hyperbolic region might play a role. To use the analysis of the characteristics, we must also assume that the Oldroyd model (2.1), or another model which responds elastically and not viscuously to step velocity data, is sufficient to predict the behavior of actual fluids in the die swell flow conditions. Joseph, Renardy, and Saut [3] show that models with Newtonian viscosity, like Jeffreys models, which smooth discontinuous initial data do not have a vorticity equation which changes type.

Another difficulty in applying the present analysis is the determination of the fluid constants appropriate for the Oldroyd model (2.1). The main

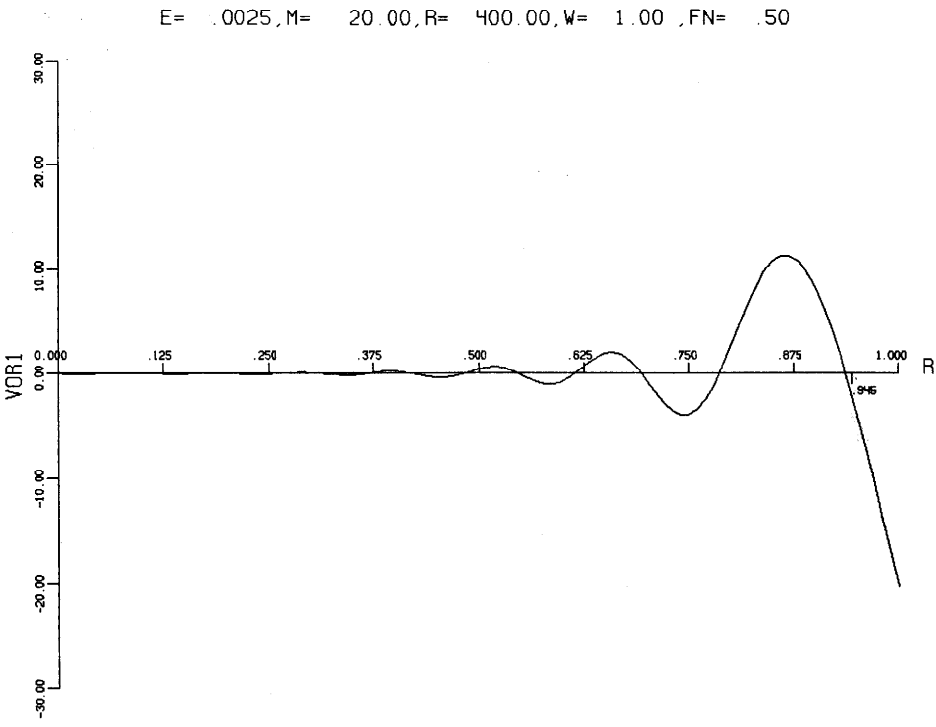

Fig. 5. Pipe flow vorticity.

difficulty is the determination of a relaxation time λ. The conclusion of Joseph, Riccius, and Arney [4] is that the wave speed of a shear wave and the measurement of a viscosity require the concept of at least two relaxation time scales (and in fact even two time scales are not enough). The shortest relaxation times give very large shear wave speeds, c, and decay quickly. They give rise to an effective Newtonian viscosity. The elasticity is associated with slower modes. Hence we have an elastic response smoothed by an effective viscosity. The elastic response has a characteristic rigidity and wave speed which appears in the tables published by Joseph, Riccius, and Arney [4]. We used these data. Even when the fast modes are dumped into an effective viscosity the relaxation spectrum cannot be well described by one relaxation time. So our choice for λ in the Maxwell model is really not possible except within wide limits.

Using the relaxation function for 1% CMC (Fig. 18 of [4]) we estimated the relaxation time in two ways. First, we used the simple formula

$$G(0) = \eta/\lambda \tag{6.7}$$

for a Maxwell model. This gives $\lambda = 0.176$ s. Second, we assumed an

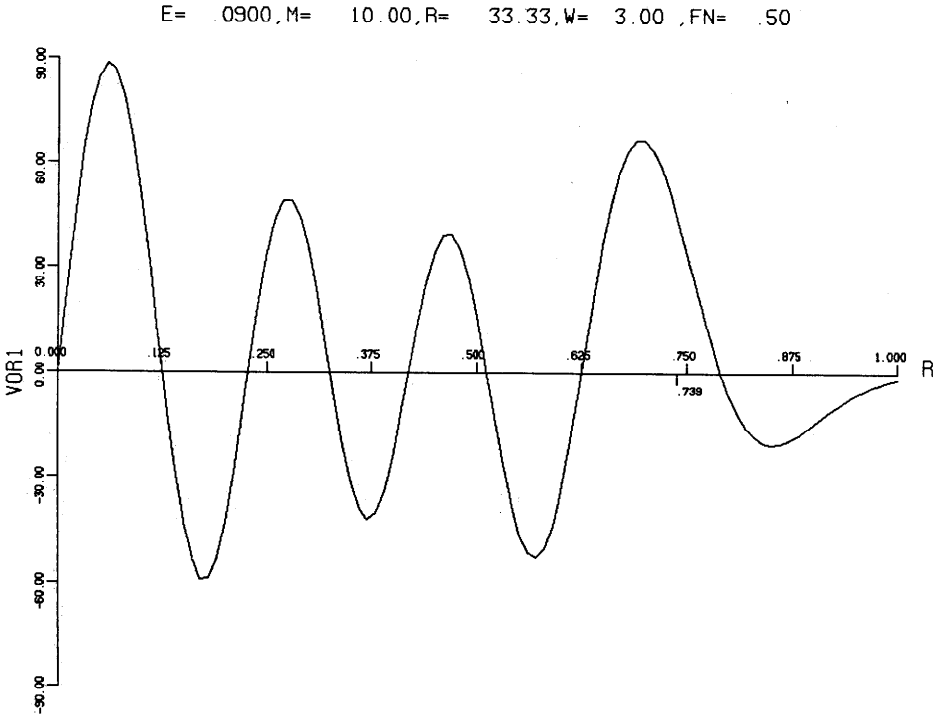

Fig. 6. Pipe flow vorticity.

exponential decay from the shear wave modulus $G(0) = G_c$ to the peak at which the instrument began to record $G(t)$. This gives $\lambda = 0.005$ s. The first estimate is too large since η includes relaxation modes that are much slower than the initial modes. Using $b = 0.05$ cm as a typical die radius for the experiments of Joseph, Matta, and Chen [2], these values of λ give

$$25 < E < 32{,}000. \tag{6.8}$$

The delayed die swell was observed to occur at about $M = 4$ for this fluid, so that (4.10) gives the hyperbolic region to be $0 < r < r^*$ where

$$0.003 < r^* < 0.10, \tag{6.9}$$

where the larger value of E gives the smaller value of r^*. For such large values of E, and of M, (4.10) may be expanded to give

$$r^* = E^{-1/2} + O(1/E). \tag{6.10}$$

This agrees with (6.9), and also shows that r^* is proportional to the radius b of the pipe for any given fluid. Thus the hyperbolic region is larger in larger pipes.

The large values of E we estimate in (6.8) for the experiments of Joseph, Matta, and Chen [2] should be related to our previous remarks on the analysis of the wavy pipe problem. The perturbation vorticity is very robust; it does not decay across the pipe. Thus the smallness of the hyperbolic region for large E may not be important since the vorticity is not damped even in the elliptic region. In addition, the Weissenberg number $W = ME^{1/2}$ is very large:

$$20 < W < 715. \tag{6.11}$$

This is beyond the range which we can compute numerically for the wavy pipe problem; and is in fact beyond the range of any reported numerical study. This indicates that any numerical study of the delayed die swell would be extremely difficult with present techniques.

Acknowledgments

This work was supported by the United States Army, Mathematics; and by the Fluid Mechanics Branch of the National Science Foundation. The work of Y.J. Yoo was supported by the Korea Science and Engineering Foundation.

References

1 J.Y. Yoo and D.D. Joseph, Hyperbolicity and change of type in the flow of viscoelastic fluids through channels. J. Non-Newtonian Fluid Mech., 19 (1985) 15–41.
2 D.D. Joseph, J. Matta and K.P. Chen, Delayed die swell. J. Non-Newtonian Fluid Mech., 24 (1987) 31–65.
3 D.D. Joseph, M. Renardy and J.C. Saut, Hyperbolicity and change of type in the flow of viscoelastic fluids. Arch. Ration. Mech. Anal., 87(3) (1985) 213–251.
4 D.D. Joseph, O. Riccius and M. Arney, Shear wave speeds and elastic moduli for different liquids; part II: experiments. J. Fluid Mech., 171 (1986) 309–338.
5 D.D. Joseph, Hyperbolic phenomena in the flow of viscoelastic fluids. In: A. Lodge, J. Nohel and M. Renardy (Eds.), Viscoelasticity and Rheology. Academic Press, 1985.

Appendix

Characteristic cones for motions perturbing uniform flow

The discussion given in section 5 of the paper by Joseph, Matta, and Chen [2] on delayed die swell makes reference to characteristic surfaces for viscoelastic fluids perturbing uniform flow. It is well known (see, for example Joseph [5]) that the linearized stress about uniform flow in the direction of the x-axis for any incompressible simple fluid is given by

$$\tau = \int_{-\infty}^{t} G[t-\tau]\, A[\boldsymbol{u}(\lambda, t)]\, \mathrm{d}\tau, \tag{A.1}$$

where

$$\lambda = \begin{vmatrix} x - U(t-\tau) \\ y \\ z \end{vmatrix},$$

$$\boldsymbol{A}[\boldsymbol{u}] = \nabla \boldsymbol{u} + \nabla \boldsymbol{u}^{\mathrm{T}}.$$

The linearized vorticity equation was given in [5] as

$$(M^2 - 1)\frac{\partial^2 \zeta}{\partial x^2} - \left(\frac{\partial^2 \zeta}{\partial y^2} + \frac{\partial^2 \zeta}{\partial z^2}\right) = \text{terms of lower derivative order} \tag{A.2}$$

where $M^2 = \rho U^2 / G(0)$. Only in the lower order terms are the details of particular models evident. For the hyperbolic analysis, however, these terms play no role.

The characteristic surfaces of (A.2), $S(x, y, z) = 0$, satisfy (see [3])

$$(M^2 - 1)(\partial S/\partial x)^2 - (\partial S/\partial y)^2 - (\partial S/\partial z)^2 = 0. \tag{A.3}$$

Provided $M > 1$, this is the usual characteristic equation for the wave equation, and a solution is the family of cones

$$\frac{1}{M^2 - 1}(x - x_0)^2 - (y - y_0)^2 - (z - z_0)^2 = 0. \tag{A.4}$$

The apex (x_0, y_0, z_0) of the cone is arbitrary, and the axis of the cone is parallel to the flow direction (the x-axis) with the cone semi-angle θ given by

$$\tan \theta = (M^2 - 1)^{-1/2}. \tag{A.5}$$